van der Waals–Like Transition in Fluidized Granular Matter

M. Argentina, M. G. Clerc, and R. Soto
Departamento de Física, Facultad de Ciencias Físicas y Matemáticas, Universidad de Chile, Casilla 487-3, Santiago, Chile
(Received 18 January 2002; published 2 July 2002)

A phase separation of fluidized granular matter is presented. Molecular dynamics simulations of a system of grains in two spatial dimensions, with a vibrating wall and without gravity, exhibit the appearance, coalescence, and disappearance of bubbles. By identifying the mechanism responsible for the phase separation, we show that the phenomenon is analogous to the spinodal decomposition of the gas-liquid transition of the van der Waals model. We have deduced a macroscopic model for the onset of phase separation which agrees quite well with molecular dynamics simulations.

DOI: 10.1103/PhysRevLett.89.044301 PACS numbers: 45.70.Mg, 05.45.–a, 64.75.+g

Granular matter, when fluidized by continuous energy injection, exhibits a variety of phenomena that resemble those of molecular fluids: patterns and instabilities appear, Rayleigh-Bénard–like convection is developed, etc. [1–3]. The main difference with molecular fluids is that, at collisions, grains dissipate kinetic energy into the internal degrees of freedom of the grains. Hence, energy must be supplied continuously to sustain a fluidized regime. Experimentally, energy is usually injected through vibrating walls or by the gravitational field.

In this Letter, we describe a new type of instability observed in fluidized granular matter, analogous to the spinodal decomposition of the gas-liquid transition in the van der Waals model [4,5]. The origin of the instability relies on the fact that for granular media the average granular temperature (defined later) is a decreasing function of the density for fixed boundary conditions. This results in negative compressibility for dissipation larger than a critical value, giving rise to a spatial instability.

We consider a two-dimensional system of grains on a horizontal surface, with friction ignored, placed in a box with a large aspect ratio (see Fig. 1). Henceforth, we will refer to the horizontal (x) and vertical (y) directions as the long and short directions, respectively; the system is periodic in the horizontal direction. The top wall reflects grains elastically while the bottom one injects energy into the system by means of vertical sinusoidal vibrations at frequency ω and amplitude A. The collisions with the wall are elastic with no tangential friction, thus conserving horizontal momentum. In the high frequency and small amplitude limit, the collisions with the wall are uncorrelated, being modeled in a stochastic way: each time a grain collides with the wall, it is reflected conserving the tangential component of the velocity, but the normal component is sorted from a Maxwellian distribution at a certain temperature that scales as $T \sim m(A\omega)^2$, m being the mass of the grains [6]. We define the granular temperature, like in molecular fluids, to be proportional to the kinetic energy per particle in the reference frame of the system. We emphasize that both collisions with the walls and between the grains conserve horizontal momentum.

The system is studied using molecular dynamics simulations of the inelastic hard sphere model (IHS) [7–9], where grains are modeled as smooth rigid disks characterized by a constant normal restitution coefficient α. Grains have only translational degrees of freedom, and there is no tangential friction between the grains at collisions. The IHS model has been widely studied and reproduces well many of the observed phenomena in granular fluids at moderate densities, where rotation is not fundamental (see, for example, [7–9]). Units are chosen such that the diameter σ and mass m of each disk is one. Also, taking the wall temperature as one, energy units are fixed. Under these conditions, the system is completely defined by the total number of grains N, the aspect ratio $\lambda = L_x/L_y \gg 1$, the global number density $n_0 = N/(L_x L_y)$, and the restitution coefficient of the grains $\alpha \equiv (1 - 2q)$; the elastic limit corresponds to $q = 0$.

At low dissipation, the granular medium develops vertical density profiles and granular temperature gradients, induced by the dissipation and the energy injection mechanism, but both fields are homogeneous in the horizontal direction. The system is hotter and less dense near the injecting wall, and colder and denser by the opposite wall, as illustrated in Fig. 1.

For larger dissipation a spatial instability is observed: the system exhibits the coexistence of two fluid phases, characterized by different densities (see Fig. 2). Initially the fluid remains horizontally homogeneous, and suddenly a bubble (defined as a low density region) appears and

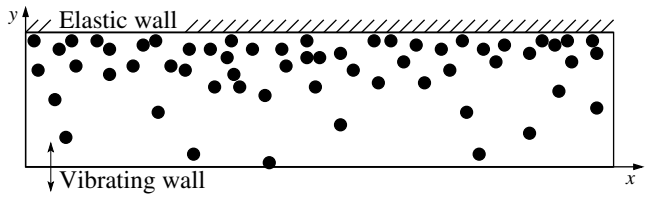

FIG. 1. Schematic representation of the studied system. Grains are placed in a horizontal box. The bottom wall is vibrating while the top one reflects grains elastically. The system is periodic in the x direction.

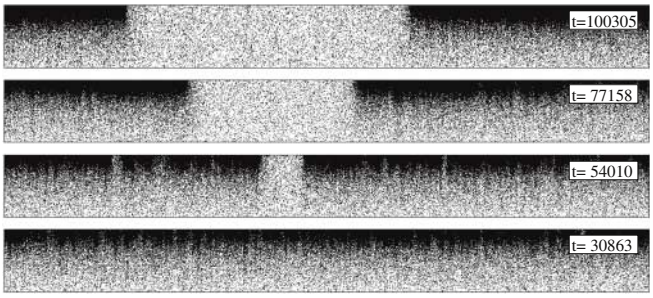

FIG. 2. Snapshots of a system with $N = 153\,600$, $\lambda = 102.4$, $n_0 = 0.15$, $L_x = 10\,240$, and $q = 0.02$. The configurations correspond to different simulation times. Each black dot represents a simulated grain and the aspect ratio has been distorted to make the system visible. The bubble appears at $t \approx 40\,000$.

grows until it achieves its final size. Afterwards, the system remains stationary with the two phases coexisting.

To characterize in more detail this instability, we analyze the temporal evolution of the vertically averaged density $\rho(x,t) = Ly^{-1} \int_0^{L_y} n(x,y,t)\, dy$, where $n(x,y,t)$ is the density field. In Fig. 3 the spatiotemporal evolution of $\rho(x,t)$ is presented. It is clearly seen that the system remains in a homogeneous state for a finite large time until the bubble is nucleated due to density fluctuations. Therefore, this homogeneous state is a metastable one. Afterwards, the bubble grows with a nearly constant velocity while two densification fronts propagate away from the bubble at a larger velocity (illustrated in Fig. 3). These fronts transport the mass lost in the bubble region. When the fronts reach the growing bubble—through the periodic boundary conditions—it is pushed inwards, leading to damped oscillations in its size. Finally, the system achieves a stationary state with one bubble.

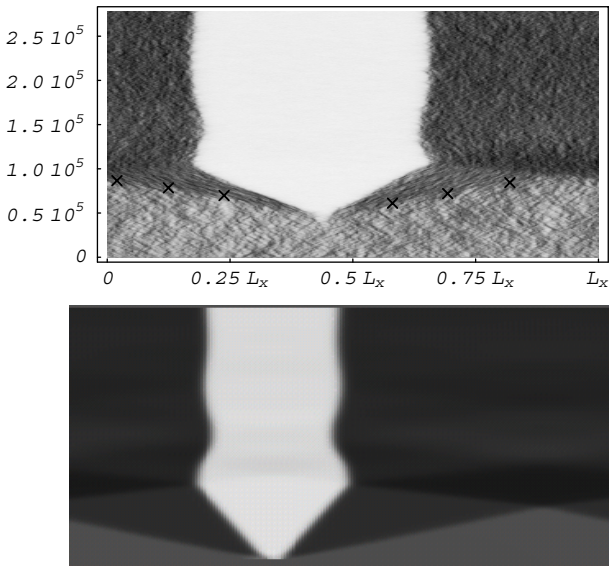

FIG. 3. Spatiotemporal evolution of the vertically averaged density, with time on the vertical axis and increasing upwards. The gray scale is proportional to density, with darker regions representing denser regions in the system. The top graph corresponds to the molecular dynamics simulation with the same parameters as in Fig. 2, where the bubble nucleation is triggered by internal noise. In the final state, the vertically averaged density of the bubble is $\rho = 0.025$, while in the dense region $\rho = 0.257$. The densification fronts are marked with lines of crosses. The bottom graph is obtained by the simulation of the model defined by Eq. (4) with $\varepsilon = -6.6 \times 10^{-4}$ and $\nu = 2$. The system size is 5400 and the total simulation is time $T = 3.5 \times 10^5$. An initial condition (with $u = 1.4 \times 10^{-2}$) that overcomes the nucleation barrier is imposed. The minimum (light gray) and maximum (dark gray) densities are $u = -2.6 \times 10^{-2}$ and $u = 2.9 \times 10^{-2}$, respectively.

The system behaves differently, according to the value of the dissipation parameter q. In Fig. 4 the spatiotemporal evolution of a system with a smaller dissipation parameter is shown. In this case four bubbles are created in the fluid with no apparent metastable time. Two of them merge into a single one, and later on the smallest one disappears or evaporates. After a transient time, the two remaining bubbles evolve slowly, one of them growing while the other one decreases. Densification fronts, created with the bubbles, are also seen.

The observed behavior is similar to the van der Waals gas-liquid transition, where for temperatures lower than the critical one, there is a density range for which the homogeneous state is unstable. Here, in the granular fluid, the control parameter is the dissipation coefficient q instead of the thermodynamic temperature.

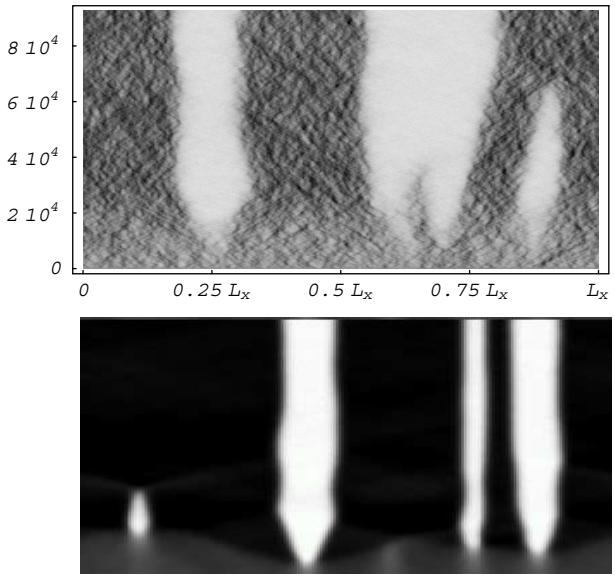

FIG. 4. The same representation as in Fig. 3, but changing the dissipation parameter to $q = 0.01$. In the final simulated state, the vertically averaged density of the bubbles is $\rho = 0.046$, while in the dense regions $\rho = 0.216$. In the bottom graph, we use the same parameters and gray scale as in Fig. 3 and the initial condition is $u = 7.4 \times 10^{-3}$. In this case there is no nucleation barrier and the initial condition used in the solution of the model is homogeneous with small fluctuations that are amplified by the instability.

The phase separation occurs over large time scales (see Figs. 3 and 4). Therefore, to describe this phenomenon, without omitting any essential physics or introducing any unnecessary complexity, one must consider the slow macroscopic variables, that is, those that also evolve over large characteristic times. Since the mass and horizontal momentum densities are the only conserved quantities, their dynamics is slow compared to the nonconserved fields, like the granular temperature of the vertical momentum. Given the aspect ratio of the simulations, the macroscopic variables have a y dependence which varies quickly and an x dependence which is slow. Hence the y-averaged variables $\rho(x,t)$ and $j(x,t)$, where ρ is the mass density and j is the horizontal momentum density, are the slow macroscopic variables that govern the dynamics of the instability. They satisfy the continuity equations

$$\partial_t \rho(x,t) = -\partial_x j(x,t)\,, \tag{1a}$$

$$\partial_t j(x,t) = -\partial_x \Phi\,, \tag{1b}$$

where Φ is the momentum flux. For the time scale we are considering, the momentum flux, granular temperature, and the other nonconserved fields are slave variables of ρ and j. Reflection invariance with respect to the y axis ($x \to -x$, $j \to -j$) and space-time translation invariance ($t \to t + t_o$, $x \to x + x_o$) imply that the momentum flux is a function of the form: $\Phi[\rho, \partial_x^{2n}\rho, j^2, \partial_x^{2n-1} j, n = 1, \ldots]$. When this flux depends only on the density, the hydrodynamic interpretation of this flux is a pressure $\{p(\rho) = \Phi[\rho]\}$. The linear dependence of Φ on $\partial_x j$ and j^2 may be understood as a viscous ($\partial_x \Phi = -\nu \partial_{xx} j$) and convective term ($\partial_x \Phi = j \partial_x j$), respectively.

Let us consider the homogeneous stationary solution $\rho = n_0$ and $j = 0$. When one neglects the viscous term, the linear behavior about this solution is described by the standard sound wave equation

$$\partial_{tt} \bar{\rho} = \frac{\partial \Phi[n_0, 0, 0, 0]}{\partial \rho}\, \partial_{xx} \overline{\rho}\,, \tag{2}$$

where $\overline{\rho} = \rho - \rho_o$. In thermodynamic equilibrium, the pressure is a monotonous increasing function of the density and the temperature [10]. The granular temperature adjusts itself to a stationary value given by the energy balance between dissipation at collisions and injection at the vibrating wall. This stationary granular temperature is a decreasing function of ρ; then the effective pressure may be a nonmonotonous function of the density, as illustrated in Fig. 5 [11]. A classical example of this behavior is the van der Waals state equation [10]: when the compressibility is negative ($\rho \partial \Phi / \partial \rho < 0$), the homogeneous state is unstable and the system presents spinodal decomposition of the gas and liquid phases.

In our model (1), the homogeneous state is unstable and spinodal decomposition takes place when $\partial \Phi[n_0, 0, 0, 0]/\partial \rho < 0$. At the onset of the instability, the first and second derivatives of Φ are small. Considering

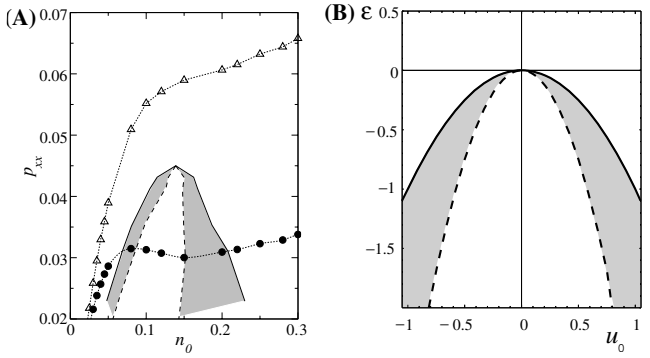

FIG. 5. (a) Phase diagram obtained from molecular dynamics simulations in tall, narrow boxes. The dotted curves correspond to the horizontal component of the pressure tensor p_{xx} for the dissipations $q = 0.0032$ (open triangles) and $q = 0.0070$ (filled circles), smaller and larger than the critical one, respectively. The second case presents a van der Waals loop. The coexistence curve (solid line) and spinodal curve (dashed line) are plotted. (b) Phase diagram obtained from the van der Waals normal form. The solid line (dashed) parabola is the coexistence (spinodal) curve. The gray region is the bistability region.

the dominant terms of Φ in j, ρ_{xx}, and j_x,

$$\Phi \approx \Phi_o + \frac{\partial \Phi}{\partial \rho}\,\bar{\rho} + \frac{\partial^2 \Phi}{\partial^2 \rho}\,\frac{\bar{\rho}^2}{2} + \frac{\partial^3 \Phi}{\partial^3 \rho}\,\frac{\bar{\rho}^3}{6} + \frac{\partial \Phi}{\partial j^2}\, j^2 + \frac{\partial \Phi}{\partial \rho_{xx}}\,\bar{\rho}_{xx} + \frac{\partial \Phi}{\partial j_x}\, j_x\,. \tag{3}$$

For the sake of simplicity, we define now $u = \overline{\rho} - \rho_M$, where ρ_M is the density at the Maxwell point (i.e., where $\partial^2 \Phi / \partial^2 \rho|_{\rho_M} = 0$) and scaling u and x, Eqs. (1), are approximated at the dominant order by the *van der Waals normal form*

$$\partial_{tt} u = \partial_{xx}(\varepsilon u + u^3 - \partial_{xx} u + \nu \partial_t u)\,, = \partial_{xx} \frac{\delta \mathcal{F}}{\delta u} + \nu \partial_{xxt} u\,, \tag{4}$$

where $\varepsilon = \partial \Phi / \partial \rho|_{\rho_M}$ is the control parameter and $\nu \partial_{xxt} u$ is a diffusion term. The variables scale as $u \sim \varepsilon^{1/2}$, $j \sim \varepsilon$, $\partial_x \sim \varepsilon^{1/2}$, $\partial_t \sim \varepsilon$, and $\nu \sim \mathcal{O}(1)$. Note that the convection term in the momentum flux ($\frac{\partial \Phi}{\partial j^2} j^2 \sim \varepsilon^2$) has been neglected in comparison with the dominant part (order $\varepsilon^{3/2}$). The sign of $\partial \Phi / \partial \rho_{xx}|_{\rho_M}$ has been chosen to be negative, in order to saturate the linear instability and to impose the existence of a global minimum for the Landau free energy $\mathcal{F} = \int dx \{\varepsilon \frac{u^2}{2} + \frac{u^4}{4} + \frac{(\partial_x u)^2}{2}\}$. For negative ε, the homogeneous solution ($u = 0$) undergoes a spatial instability, characterized by the appearance of equally distributed bubbles. Later on, the closest bubbles merge into a larger one, as a consequence of a coalescence process. Subsequently, bubble dynamics is led by the interaction mediated by waves (see Fig. 4). The above dynamics is a consequence of the system's tendency to minimize its free energy. With periodic boundary conditions, the

global minimum is a unique bubble, as the solution shown in Fig. 3. Further work on this coarsening process is in progress.

We emphasize that the system described by model (4) has the classical phase diagram, with coexistence and spinodal curves [4]; as those observed in binary fluids, binary alloys, and ^{3}He-^{4}He mixtures, to mention a few examples (see [5] and references cited therein).

In the bistability region, i.e., in the region bounded by the spinodal and coexistence curves (see Fig. 5), the homogeneous state is stable. Nevertheless, a finite fluctuation that overcomes the nucleation barrier gives rise to a bubble along with two *state waves (densification waves),* which propagate away from the bubble as a result of mass conservation (see Fig. 3). Because of the periodic boundary conditions, the waves eventually collide with the bubble, making its size oscillate. Afterwards, the oscillations are damped by viscosity and the final state is a single bubble at rest.

The model (4) implies that for global densities smaller than the Maxwell point density ($u < 0$), dense regions (instead of low density regions) can nucleate. We have checked in molecular dynamics simulations that this is indeed the case. For $N = 153\,600$, $q = 0.02$, and $L_y = 100$ dense regions nucleate for densities between $n_0 = 0.033$ and $n_0 = 0.08$. These regions evolve in a similar way to bubbles; that is, they interact through waves, merge, and eventually disappear.

The van der Waals normal form is based on the hypothesis that the momentum flux Φ as a function of density has an inflection point. To check this, we have performed molecular dynamics simulations of the IHS system in narrow boxes ($L_x \ll L_y$) to prevent the development of the spatial instability. We compute the horizontal momentum flux (x-x component of the pressure tensor, p_{xx}), averaged over the vertical direction for different values of the global density n_0 and the dissipation coefficient q. We obtain that indeed Φ has a negative compressibility region (see Fig. 5) with a critical point located at $q \approx 0.0047$ and $n_0 \approx 0.14$.

The model (4) can also be derived from a hydrodynamic description of granular fluids. Further work in this direction is in progress.

In summary, we have studied a phase separation phenomenon in fluidized granular matter. Molecular dynamics simulations of a grain system in two dimensions, with a vibrating wall and no gravity, exhibit appearance, coalescence, and disappearance of low density regions (bubbles). Rarefaction and densification density waves lead the bubble dynamics. The mechanism of phase separation is triggered by a negative compressibility which is, in turn, a result of the fact that for granular media the granular temperature is a decreasing function of the density.

Close to the transition, the system is described by the van der Waals normal form (4). This model describes quite well the results from molecular dynamics simulations. The phase separation is analog to the spinodal decomposition of the gas-liquid transition of the van der Waals model, but the transient evolution of the system is led by state waves.

The van der Waals instability should be observed independently of the peculiarities of the energy injection mechanism or of its stochastic modelization, as long as the particle collisions with the wall conserve horizontal momentum. It should also be observed in the presence of a small gravitational field either by inclining the table slightly or by placing the system vertically with characteristic injected energy much larger than the gravitational potential energy [$m(A\omega)^2 \gg mgL_y$]. In both possible generalizations, the general theoretical framework continues to be valid, and preliminary numerical simulations confirm it (in preparation).

The authors thank P. Cordero, D. Risso, and E. Tirapegui for fruitful discussions. The simulation software developed at INLN, France, has been used for the simulations of model (4). M. G. C. and R. S. appreciate the support of *Programa de inserción de científicos chilenos* of Fundación Andes and the support of FONDAP Grant No. 11980002. M. A. and R. S. are thankful for the support of the FONDECYT Projects No. 30000017 and No. 1010416, respectively.

[1] P. B. Umbanhowar, F. Melo, and H. L. Swinney, Nature (London) **382**, 793 (1996).
[2] R. Ramírez, D. Risso, and P. Cordero, Phys. Rev. Lett. **85**, 1230 (2000).
[3] Y. Forterre and O. Pouliquen, Phys. Rev. Lett. **86**, 5886 (2001).
[4] J. W. Cahn and J. E. Hilliard, J. Chem. Phys. **28**, 258 (1958).
[5] J. D. Gunton, M. San Miguel, and P. S. Sanhi, in *Phase Transitions and Critical Phenomena,* edited by D. Domb and J. L. Lebowitz (Academic Press, London, 1983), Vol. 8, pp. 267–466.
[6] S. Warr and J. M. Huntley, Phys. Rev. E **52**, 5596 (1995).
[7] I. Goldhirsch and G. Zanetti, Phys. Rev. Lett. **70**, 1619 (1993).
[8] P. Zamankhan, A. Mazouchi, and P. Sarkomaa, Appl. Phys. Lett. **71**, 3790 (1997).
[9] D. C. Rapaport, Physica (Amsterdam) **249A**, 232 (1998).
[10] L. D. Landau and E. M. Lifshitz, *Statistical Physics* (Pergamon Press, New York, 1969).
[11] This mechanism is similar to the one that gives rise to the clustering phenomenon presented in Ref. [7]. Nevertheless, in the case presented in the reference, the granular temperature is not a slave variable.